Nonlinear fundamental photothermal response in three-dimensional geometry: Theoretical model

Andreas Mandelis
Photothermal and Optoelectronic Diagnostics Laboratories, Department of Mechanical and Industrial Engineering, University of Toronto, 5 King's College Road, Toronto, Ontario M5S 3G8, Canada

Alex Salnick,[a] Jon Opsal, and Allan Rosencwaig
Therma-Wave, Incorporated, 1250 Reliance Way, Fremont, California 94539

(Received 12 May 1998; accepted for publication 3 November 1998)

A general three-dimensional theoretical model for fundamental and harmonic response generation as a result of periodic heating of a system consisting of a nonlinear layer with temperature-dependent thermal conductivity and specific heat and a linear substrate is developed. Analysis of the fundamental component of the surface temperature shows that the nonlinear thermal conductivity alone does not affect the phase of the thermal-wave field. The efficiency of the thin nonlinear layer as an energy conversion filter that drives the harmonic response of the substrate is shown by the analysis of the limiting cases of the theoretical model. © *1999 American Institute of Physics.* [S0021-8979(99)10403-1]

I. INTRODUCTION

Over the past two decades, thermal waves have been extensively used to study the optical, thermal, and electronic properties of various materials.[1,2] As was first noted by Opsal *et al.*,[3] in these thermal-wave experiments dc and ac temperature excursions can range from several degrees to several hundred degrees depending on the sample's thermal properties. With such wide temperature variations, the dependence on temperature of the thermal, optical, and elastic parameters of the thermally excited medium has to be taken into account in the corresponding theoretical models.

Growing interest in nonlinear photothermal phenomena has been motivated by several experimental studies which demonstrated that thermal-wave second harmonic detection can provide better contrast in photothermal microscopy.[4,5] Rajakarunanayake and Wickramasinghe[4] first described nonlinear photothermal deflection imaging experimentally, where the pump beam is modulated at angular frequency ω and the signal is detected at 2ω. Wetsel and Spicer[5] also demonstrated the nonlinear effect in photothermal deflection imaging, and a theoretical model with special nonlinear boundary conditions was developed. A more general theory with nonlinear bulk thermal parameters was proposed by Doka *et al.*[6] Wang and Li[7] further developed a photothermal inspection technique using the photothermal infrared radiometric scheme to detect the second-harmonic response. Finally, Gusev *et al.*[8–10] published several papers with theoretical analyses of the thermal-wave second harmonic generation induced by the modulated heating of media with temperature-dependent thermophysical properties. The common feature of all the previous theoretical and experimental nonlinear photothermal studies is that only second-harmonic detection has been formulated, and only in one-dimensional geometry. To the best of our knowledge, no experimental works or theoretical models have addressed the general boundary value problem of the full nonlinear photothermal response of an overlayer on a linear substrate. Yet, the development of such a theoretical framework is of practical interest for thermal-wave nondestructive evaluation (NDE) studies of materials exhibiting a very strong nonlinear behavior, such as, for example, tungsten. Another important fact is that modern thermal-wave NDE experiments employ submicron spatial resolution and very high excitation power densities (on the order of MW/cm^2), thus requiring an adequate three-dimensional theoretical treatment. Besides the practical importance of a rigorous three-dimensional (3D) exact photothermal nonlinear theory, there is intrinsic value in the physical insights one obtains when studying the extraordinary behavior of thermally nonlinear media under intense photothermal-wave excitation.

In this article we develop a general 3D theoretical model for the fundamental and harmonic response generation of arbitrary order as a result of periodic heating of a layered structure consisting of an upper thin nonlinear layer in intimate contact with a semi-infinite linear substrate. The upper layer is assumed to exhibit temperature-dependent thermal conductivity and specific heat.

II. THEORETICAL MODEL

A. The thermal-wave problem of a nonlinear layer on semi-infinite linear substrate

We start with the most general case where a layer with nonlinear thermophysical properties overlies a semi-infinite linear substrate in intimate physical and thermal contact. The assumed theoretical geometry is shown in Fig. 1. The upper layer is assumed to be fully opaque to the incident laser radiation.

A pair of conventional heat conduction equations can be written, one for the top layer with nonconstant, temperature-

[a]Electronic mail: asalnik@thermawave.com

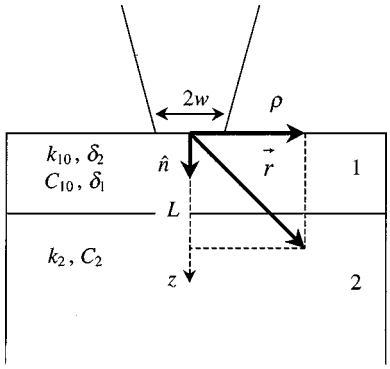

FIG. 1. Schematic representation of the two-layer sample consisting of a nonlinear layer and a semi-infinite linear substrate. The layer is photothermally excited by a Gaussian laser beam of spot size w, intensity modulated at angular frequency ω.

dependent thermophysical parameters and another for the linear substrate with boundary conditions of continuity of heat flux and temperature at the interfaces

$$\nabla[k_1(T_1)\nabla T_1]-C_1(T_1)\frac{\partial T_1}{\partial t}=0, \quad 0\leqslant z\leqslant L, \tag{1a}$$

with the complete combined dc and ac boundary condition at $z=0$:

$$-k_1\hat{n}\nabla T_1|_{z=0}=\tfrac{1}{2}I_\omega(1+e^{i\omega t}), \tag{1b}$$

and the continuity boundary conditions,

$$k_1\hat{n}\nabla T_1|_{z=L}=k_2\hat{n}\nabla T_2|_{z=L}, \tag{1c}$$

$$T_1(\mathbf{r},t)|_{z=L}=T_2(\mathbf{r},t)|_{z=L}, \tag{1d}$$

at $z=L$. Here $\hat{n}$ is the unit vector normal to the surface plane $z=0$ in the direction inward to the material volume under consideration. For bounded behavior of the thermal-wave field $T_2(\mathbf{r},t)$ it is required that

$$T_2(\mathbf{r},t)|_{r\to\infty}=0. \tag{1e}$$

The response of the linear substrate is governed by

$$\nabla^2 T_2-\frac{1}{\alpha_2}\frac{\partial T_2}{\partial t}=0. \tag{1f}$$

In the boundary-value problem of Eqs. (1a)–(1f), k_1 is the upper layer thermal conductivity, C_1 is the product of the layer density and the specific heat, I_ω is the intensity of the pump-beam irradiation modulated at the angular frequency ω, and α_2 is the substrate thermal diffusivity $\alpha_2=k_2/C_2$.

Let us suppose that external heating produces dc and modulated increases in layer temperature T_{1d} and T_{1a}, respectively,

$$T_1(\mathbf{r},t)=T_{1d}(\mathbf{r})+T_{1a}(\mathbf{r},t). \tag{2}$$

Furthermore, the assumption is made that

$$C_1(T)\cong C_{10}(T_{1d})+\left(\left.\frac{\partial C_1}{\partial T}\right|_{T=T_{1d}}\right)T_{1a}$$
$$\equiv C_{10}[1+\delta_1 T_1(\mathbf{r},t)] \tag{3a}$$

and

$$k_1(T)\cong k_{10}(T_{1d})+\left(\left.\frac{\partial k_1}{\partial T}\right|_{T=T_{1d}}\right)T_{1a}$$
$$\equiv k_{10}[1+\delta_2 T_1(\mathbf{r},t)] \tag{3b}$$

adequately describe the behavior of the specific heat and thermal conductivity of the layer in the temperature interval of interest, where, by definition,

$$\delta_1\equiv\frac{1}{C_1(T_{1d})}\left(\left.\frac{dC_1(T_1)}{dT_1}\right|_{T_1=T_{1d}}\right)$$
$$=\frac{d}{dT_1}\ln[C_1(T_1)]\Big|_{T_1=T_{1d}} \tag{3c}$$

and

$$\delta_2\equiv\frac{1}{k_1(T_{1d})}\left(\left.\frac{dk_1(T_1)}{dT_1}\right|_{T_1=T_{1d}}\right)$$
$$=\frac{d}{dT_1}\ln[k_1(T_1)]\Big|_{T_1=T_{1d}}. \tag{3d}$$

Under the conditions of Eqs. (2) and (3), Eq. (1a), subject to boundary condition (1b) and under the uniform background (dc) temperature conditions $\nabla T_{1d}=\nabla^2 T_{1d}=0$, transforms to

$$\nabla^2 T_1(\mathbf{r},t)-\frac{1}{\alpha_{10}}\frac{\partial}{\partial T}T_1(\mathbf{r},t)$$
$$=-\frac{1}{2}\left(\delta_2\nabla^2-\frac{\delta_1}{\alpha_{10}}\frac{\partial}{\partial t}\right)T_1^2(\mathbf{r},t), \quad 0\leqslant z\leqslant L, \tag{4a}$$

where $\alpha_{10}=k_{10}/C_{10}$ is the unperturbed thermal diffusivity of the upper layer at temperature T_{1d}. For the linear substrate,

$$\nabla^2 T_2(\mathbf{r},t)-\frac{1}{\alpha_2}\frac{\partial}{\partial t}T_2(\mathbf{r},t)=0, \quad L\leqslant z<\infty. \tag{4b}$$

Nonlinear boundary conditions can be written from Eqs. (1b) and (1c) as follows:

$$-k_{10}\frac{\partial}{\partial z}[T_1(\mathbf{r},t)+\tfrac{1}{2}\delta_2 T_1^2(\mathbf{r},t)]|_{z=0}=\tfrac{1}{2}I_\omega(1+e^{i\omega t}), \tag{5a}$$

and

$$k_{10}\frac{\partial}{\partial z}[T_1(\mathbf{r},t)+\tfrac{1}{2}\delta_2 T_1^2(\mathbf{r},t)]|_{z=L}=k_2\left.\frac{\partial}{\partial z}T_2(\mathbf{r},t)\right|_{z=L}. \tag{5b}$$

Note that both the temperature-dependent specific heat and the conductivity contribute to nonlinear terms in the nonlinear heat conduction equation (4a), whereas only $k_1(T)$ contributes to the nonlinearity in the boundary conditions, Eqs. (5).

Since there is intimate contact between the nonlinear layer and the substrate at the interface $z=L$, and since the nonlinear layer will produce multiple harmonics of the fundamental, the substrate will also exhibit multiple harmonics due to the thermal-wave field conducted past the interface. Therefore, let the solution to Eqs. (4) be in the form of the superpositions,

$$T_1(\mathbf{r},t)=\sum_{n=-\infty}^{\infty} T_{1n}(\mathbf{r})e^{in\omega t}, \tag{6}$$

and

$$T_2(\mathbf{r},t)=\sum_{m=-\infty}^{\infty} T_{2m}(\mathbf{r})e^{im\omega t}. \tag{7}$$

Correspondingly, upon insertion of Eqs. (6) and (7), Eqs. (4a) and (4b) become

$$\sum_{n=-\infty}^{\infty}\left\{\nabla^2 T_{1n}(\mathbf{r})-\frac{in\omega}{\alpha_{10}}T_{1n}(\mathbf{r})\right\}e^{in\omega t} =-\frac{1}{2}\left(\delta_2\nabla^2-\frac{\delta_1}{\alpha_{10}}\frac{\partial}{\partial t}\right)\left(\sum_{n=-\infty}^{\infty} T_{1n}(\mathbf{r})e^{in\omega t}\right)^2, \tag{8a}$$

and

$$\sum_{m=-\infty}^{\infty}\left\{\nabla^2 T_{2m}(\mathbf{r})-\frac{im\omega}{\alpha_2}T_{2m}(\mathbf{r})\right\}e^{im\omega t}=0. \tag{8b}$$

The representation of the foregoing summations to include negative harmonics is preferred in order to simplify the calculation of complex quantities and harmonic orders. In identifying the boundary-value problem for each harmonic order, a redefinition of the amplitudes $T_{ij}(\mathbf{r})$ is made in what follows, based on

$$\sum_{n=-\infty}^{\infty} e^{in\omega t}=1+2\sum_{n=0}^{\infty}\cos(n\omega t).$$

B. Harmonic order boundary-value problem formalism

The exact solution of the system of master equations (8), coupled through boundary conditions (5), can be conveniently decomposed into an infinite set of nonlinear equations for each modulation frequency harmonic order, including the fundamental, ω, $n=1$, and the background dc term, $n=0$. Experimentally, the fundamental is the most important term, as it can be directly monitored through a conventional spectral filter arrangement, such as a lock-in analyzer.

1. n=0 (dc) term

In the case of $n=0$ the dc component of problem (8) transforms to the following set of equations:

$$\nabla^2[T_{10}(\mathbf{r})+\tfrac{1}{2}\delta_2 T_{10}^2(\mathbf{r})]=0, \tag{9a}$$

$$\nabla^2 T_{20}(\mathbf{r})=0. \tag{9b}$$

The boundary conditions, Eqs. (5), can also be spectrally decomposed into summations of the dc term, the fundamental, and the harmonics. For the dc term we obtain

$$-k_{10}\frac{\partial}{\partial z}[T_{10}(\mathbf{r})+\tfrac{1}{2}\delta_2 T_{10}(\mathbf{r})]\big|_{z=0}=\tfrac{1}{2}I_\omega, \tag{9c}$$

and

$$k_{10}\frac{\partial}{\partial z}[T_{10}(\mathbf{r})+\tfrac{1}{2}\delta_2 T_{10}(\mathbf{r})]\big|_{z=L}=k_2\frac{\partial}{\partial z}T_{20}(\mathbf{r})\big|_{z=L}, \tag{9d}$$

for heat-flux continuity, as well as

$$T_{10}(\mathbf{r})+\tfrac{1}{2}\delta_2 T_{10}(\mathbf{r})\big|_{z=L}=T_{20}(\mathbf{r})\big|_{z=L} \tag{9e}$$

for temperature continuity at $z=L$. To simplify the notation, we use the following definition:

$$F_{10}(\mathbf{r})\equiv T_{10}(\mathbf{r})+\tfrac{1}{2}\delta_2 T_{10}^2(\mathbf{r}); \tag{10}$$

then the system of Eqs. (9a)–(9e) becomes

$$\nabla^2 F_{10}(\mathbf{r})=0, \tag{11a}$$

with the boundary condition at $z=0$,

$$-k_{10}\frac{\partial}{\partial z}F_{10}(\mathbf{r})\bigg|_{z=0}=\tfrac{1}{2}I_\omega=\tfrac{1}{2}I_0 e^{-\rho^2/w^2}, \tag{11b}$$

assuming a Gaussian laser beam source of spot size w, and $r^2=\rho^2+z^2$ (Fig. 1). Also at $z=L$:

$$k_{10}\frac{\partial}{\partial z}F_{10}(\mathbf{r})\bigg|_{z=L}=k_2\frac{\partial}{\partial z}T_{20}(\mathbf{r})\bigg|_{z=L}, \tag{11c}$$

$$F_{10}(\mathbf{r})_{z=L}=T_{20}(\mathbf{r})\big|_{z=L}. \tag{11d}$$

The partial differential boundary-value problem of Eqs. (9b)–(9e) and (11a)–(11d) can be solved by use of their Fourier–Bessel (Hankel) transforms, reflecting the cylindrical symmetry of the geometry of Fig. 1:

$$\tilde{\tau}_{20}(\lambda,z)=\int_0^\infty J_0(\lambda\rho)T_{20}(\rho,z)\rho d\rho, \tag{12}$$

and

$$\tilde{f}_{10}(\lambda,z)=\int_0^\infty J_0(\lambda\rho)F_{10}(\rho,z)\rho d\rho. \tag{13}$$

Substituting the Hankel transforms in Eqs. (9b) and (11a) gives, in cylindrical coordinates, the following solutions:

$$\tilde{f}_{10}(\lambda,z)=A(\lambda)e^{-\lambda z}+B(\lambda)e^{\lambda z},\quad 0\leqslant z\leqslant L, \tag{14}$$

$$\tilde{\tau}_{20}(\lambda,z)=C(\lambda)e^{-\lambda(z-L)},\quad z\geqslant L. \tag{15}$$

Performing the Hankel transformation of boundary conditions (11b)–(11d) we obtain the algebraic system,

$$k_{10}\lambda[A(\lambda)-B(\lambda)]=I_0 w^2 e^{-\lambda^2 w^2/4}, \tag{16a}$$

$$k_{10}[A(\lambda)e^{-\lambda L}-B(\lambda)e^{\lambda L}]=k_2 C(\lambda), \tag{16b}$$

$$A(\lambda)e^{-\lambda L}+B(\lambda)e^{\lambda L}=C(\lambda). \tag{16c}$$

Solving this system of equations and substituting back in the inverse Hankel transforms of Eqs. (12) yield the solution for the dc temperature rise due to the Gaussian laser-beam heating of the composite layer of Fig. 1:

$$F_{10}(\rho,z)=\frac{I_0 w^2}{k_{10}}\int_0^\infty\left(\frac{e^{-\lambda z}+\gamma_{21}e^{-\lambda(2L-z)}}{1-\gamma_{21}e^{-2\lambda L}}\right)\times e^{-\lambda^2 w^2/4}J_0(\lambda\rho)d\lambda,\quad 0\leqslant z\leqslant L, \tag{17}$$

and

$$T_{20}(\rho,z)=\frac{2I_0 w^2}{k_{10}(1+b_{21})}\int_0^\infty\left(\frac{e^{-\lambda z}}{1-\gamma_{21}e^{-2\lambda L}}\right)\times e^{-\lambda^2 w^2/4}J_0(\lambda\rho)d\lambda,\quad L\leqslant z<\infty, \tag{18}$$

where $b_{21}=k_2/k_{10}$ is the dc-field thermal coupling coefficient between the upper layer and the substrate, and $\gamma_{21}\equiv(1-b_{21})/(1+b_{21})$.

Finally, from the defining equation (10), the dc temperature increase of the nonlinear thin layer is

$$T_{10}(\rho,z)=\frac{1}{\delta_2}(\sqrt{1+2\delta_2F_{10}(\rho,z)}-1). \tag{19}$$

Note that this dc term is affected by the temperature-dependent thermal conductivity only. It is easy to see that in the limit $\delta_2F_{10}(\rho,z)\ll 1$ $T_{10}(\rho,z)\to F_{10}(\rho,z)$, the solution for a linear medium given by Eq. (17). This is, indeed, the solution of Eq. (10) for $\delta_2T_{10}^2\ll 1$ (which implies $\delta_2=0$).

2. $n=1$ *(fundamental) term*

Proceeding as in the $n=0$ case with Eqs. (8a) and (8b) and boundary conditions (5a) and (5b), and making use of the superposition principle of the diffusion-wave field's $n=1$ term of Eq. (8a), we obtain the equivalent system of two equations,

$$\nabla^2H_1(\mathbf{r})-\sigma_{11}^2H_1(\mathbf{r})=0,\quad 0\leqslant z\leqslant L, \tag{20a}$$

$$\nabla^2H_2(\mathbf{r})-\left(\frac{\delta_2}{\delta_1}\right)\sigma_{11}^2H_2(\mathbf{r})=0,\quad 0\leqslant z\leqslant L, \tag{20b}$$

for the upper layer, where

$$H_1(\mathbf{r})\equiv T_{11}(\mathbf{r})+(\delta_1+\delta_2)T_{10}(\mathbf{r})T_{11}(\mathbf{r}), \tag{21a}$$

and

$$H_2(\mathbf{r})\equiv T_{10}(\mathbf{r})T_{11}(\mathbf{r}). \tag{21b}$$

For the substrate

$$\nabla^2T_{21}(\mathbf{r})-\sigma_{21}^2T_{21}(\mathbf{r})=0,\ L\leqslant z<\infty. \tag{22}$$

Here, $T_{11}(\mathbf{r})$ and $T_{21}(\mathbf{r})$ are defined in the context of master equations (8a) and (8b) subject to the following heat-flux boundary conditions:

$$-k_{10}\frac{\partial}{\partial z}H_1(\mathbf{r})\bigg|_{z=0}+\delta_1k_{10}\frac{\partial}{\partial z}H_2(\mathbf{r})\bigg|_{z=0}=\frac{1}{2}I_\omega, \tag{23a}$$

$$k_{10}\frac{\partial}{\partial z}H_1(\mathbf{r})\bigg|_{z=L}-\delta_1k_{10}\frac{\partial}{\partial z}H_2(\mathbf{r})\bigg|_{z=L}=k_2\frac{\partial}{\partial z}T_{21}(\mathbf{r})\bigg|_{z=L}, \tag{23b}$$

and the temperature continuity boundary condition,

$$H_1(\mathbf{r})-\delta_1H_2(\mathbf{r})|_{z=L}=T_{21}(\mathbf{r})|_{z=L}. \tag{23c}$$

The following definitions of the thermal wave vectors were also made:

$$\sigma_{11}^2=i\omega/\alpha_{10},\quad \sigma_{21}^2=i\omega/\alpha_2. \tag{24}$$

Hankel transforms of Eqs. (20) and (22) yield

$$\tilde{h}_1(\lambda,z)=A(\lambda)e^{-\xi_{11}z}+B(\lambda)e^{\xi_{11}z}, \tag{25}$$

$$\tilde{h}_2(\lambda,z)=C(\lambda)e^{-q_{11}z}+D(\lambda)e^{q_{11}z}, \tag{26}$$

and

$$\tilde{\tau}_{21}(\lambda,z)=E(\lambda)e^{-\xi_{21}(z-L)}, \tag{27}$$

where

$$\xi_{11}\equiv\sqrt{\lambda^2+\sigma_{11}^2},\quad q_{11}\equiv\sqrt{\lambda^2+(\delta_2/\delta_1)\sigma_{11}^2},$$
$$\xi_{21}\equiv\sqrt{\lambda^2+\sigma_{21}^2}. \tag{28}$$

After Hankel transformations of the boundary conditions we obtain the algebraic system,

$$k_{10}\{\xi_{11}[A(\lambda)-B(\lambda)]-\delta_1q_{11}[C(\lambda)-D(\lambda)]\}=I_0w^2e^{-\lambda^2w^2/4}, \tag{29a}$$

$$k_{10}\{\xi_{11}[A(\lambda)e^{-\xi_{11}L}-B(\lambda)e^{\xi_{11}L}]-\delta_1q_{11}[C(\lambda)e^{-q_{11}L}-D(\lambda)e^{q_{11}L}]\}=k_2\xi_{21}E(\lambda), \tag{29b}$$

$$A(\lambda)e^{-\xi_{11}L}+B(\lambda)e^{\xi_{11}L}-\delta_1[C(\lambda)e^{-q_{11}L}+D(\lambda)e^{q_{11}L}]=E(\lambda). \tag{29c}$$

Two more equations are required to solve the system (A, B, C, D, and E). From the defining Eqs. (21a) and (21b) we find

$$H_1(\rho,z)=T_{11}(\rho,z)+(\delta_1+\delta_2)H_2(\rho,z). \tag{30}$$

Unfortunately, letting $T_{11}(\rho,z)=H_2(\rho,z)/T_{10}(\rho,z)$ does not provide a second equation between $A(\lambda)$ and $B(\lambda)$, as the Hankel transform of the ratio of two functions is not equal to the ratio of Hankel transforms. Therefore, a stepwise approach must be taken with Eq. (30) in order to solve for $T_{11}(\rho,z)$.

It should be recalled that the original boundary-value problems for the two layers, linked with the interfacial ($z=L$) boundary conditions and leading to master equations (8a) and (8b), have resulted in the infinite number of boundary-value problems ($n=0$, $n=1$, $n=2$, etc.), the superposition of which is equivalent to the original problems under the first-order Taylor expansions for $k_1(T)$ and $C_1(T)$.

C. Stepwise approximation

The stepwise approach to Eq. (30), akin to the multiple-order Born approximation familiar from scattering field theory, differs from classical perturbation treatments in that there is no small parameter involved, powers of which are equated. The field $T_{11}(\rho,z)$ in Eq. (30) can be determined to any degree of approximation by making sequential approximations of the value of the field $H_2(\rho,z)$, which, in turn, impact the calculation of the integration constants $C(\lambda)$ and $D(\lambda)$ in Eq. (26).

As the first approximation, letting $H_2(\rho,z)=0$ in Eq. (30) we obtain from its Hankel transform

$$\int_0^\infty[C(\lambda)e^{-q_{11}z}+D(\lambda)e^{q_{11}z}]J_0(\lambda\rho)\lambda\,d\lambda=0. \tag{31}$$

This equation implies that the expression in brackets within the integrand must be identically zero for all values of z. Therefore, taking $z=0$, L, and solving for the coefficients C and D gives $C(\lambda)=D(\lambda)=0$. Equations (29a)–(29c) now can be unambiguously solved and they give

$$A(\lambda)=\frac{g(\lambda)}{1-\Gamma_{21}(\lambda)e^{-2\xi_{11}L}}, \tag{32}$$

$$B(\lambda)=\frac{\Gamma_{21}g(\lambda)e^{-2\xi_{11}L}}{1-\Gamma_{21}(\lambda)e^{-2\xi_{11}L}}, \tag{33}$$

and

$$E(\lambda)=\frac{2g(\lambda)e^{-\xi_{11}L}}{(1-B_{21})(1-\Gamma_{21}(\lambda)e^{-2\xi_{11}L})}, \tag{34}$$

where the following definitions in Hankel space were made:

$$g(\lambda)\equiv\frac{I_0w^2}{k_{10}\xi_{11}}e^{-\lambda^2w^2/4}, \tag{35}$$

and

$$B_{21}(\lambda)\equiv b_{21}\left(\frac{\xi_{21}(\lambda)}{\xi_{11}(\lambda)}\right), \quad \Gamma_{21}(\lambda)\equiv\frac{1-B_{21}(\lambda)}{1+B_{21}(\lambda)}. \tag{36}$$

Therefore, from Eqs. (25) and (30), the inverse Hankel transform gives the first approximation to the stepwise treatment of the fundamental component $T_{11}(\rho,z,\omega)$ of the nonlinear thermal-wave field:

$$\begin{aligned}T_{11}(\rho,z,\omega)&\cong H_{10}(\rho,z,\omega)\\&=\frac{I_0W^2}{k_{10}}\int_0^\infty\left(\frac{e^{-\xi_{11}z}+\Gamma_{21}(\lambda)e^{-\xi_{11}(2L-z)}}{\xi_{11}(\lambda)(1-\Gamma_{21}(\lambda)e^{-2\xi_{11}L})}\right)\\&\quad\times J_0(\rho\lambda)e^{-\lambda^2w^2/4}\lambda d\lambda.\end{aligned} \tag{37}$$

This equation is the linear (exact) solution to the $n=1$ boundary-value problem in the upper thin layer when one sets $\delta_1=\delta_2=0$. Therefore, to the extent of the validity of the first stepwise approximation, setting $H_2(\rho,z)=0$ is equivalent to a conventional perturbation treatment of the nonlinear thermal-wave problem in the upper layer, where the small-magnitude parameters δ_1 and δ_2 can be set equal to zero and the formalism produces the same results.

As the second approximation, from the definition of $H_2(\mathbf{r})$, Eq. (21b),

$$H_2(\rho,z)=T_{10}(\rho,z)T_{11}(\rho,z)\cong T_{10}(\rho,z)H_{10}(\rho,z), \tag{38}$$

we obtain the Hankel transforms

$$\tilde{h}_2(\lambda,0)=\int_0^\infty f(\rho,0)J_0(\lambda\rho)\rho d\rho=C(\lambda)+D(\lambda), \tag{39a}$$

and

$$\tilde{h}_2(\lambda,L)=\int_0^\infty f(\rho,L)J_0(\lambda\rho)\rho d\rho=C(\lambda)e^{-q_{11}L}+D(\lambda)e^{q_{11}L}, \tag{39b}$$

where $f(\rho,0)\equiv T_{10}(\rho,0)H_{10}(\rho,0)$, and $f(\rho,L)\equiv T_{10}(\rho,L)H_{10}(\rho,L)$.

Solving Eqs. (39a) and (39b) for $C(\lambda)$ and $D(\lambda)$,

$$C(\lambda)=\frac{1}{1-e^{-2q_{11}L}}[\tilde{h}_2(\lambda,0)-\tilde{h}_2(\lambda,L)e^{-q_{11}L}], \tag{40}$$

and

$$D(\lambda)=\frac{e^{-q_{11}L}}{1-e^{-2q_{11}L}}[\tilde{h}_2(\lambda,L)-\tilde{h}_2(\lambda,0)e^{-q_{11}L}]. \tag{41}$$

Finally, solution of the system of Eqs. (29) now becomes possible, giving

$$\begin{aligned}A(\lambda)=\frac{1}{1-\Gamma_{21}(\lambda)e^{-2\xi_{11}L}}&\left\{g(\lambda)+\frac{\delta_1}{1+B_{21}(\lambda}\left[\left(\frac{q_{11}}{\xi_{11}}\right)\right.\right.\\&\times[M(\lambda)-N(\lambda)e^{-\xi_{11}L}]\\&\left.\left.+B_{21}(\lambda)\tilde{h}_2(\lambda,L)e^{-\xi_{11}L}\right]\right\},\end{aligned} \tag{42}$$

$$\begin{aligned}B(\lambda)=\frac{\Gamma_{21}(\lambda)e^{-2\xi_{11}L}}{1-\Gamma_{21}(\lambda)e^{-2\xi_{11}L}}&\left\{g(\lambda)e^{-\xi_{11}L}+\delta_1\left[\left(\frac{q_{11}}{\xi_{11}}\right)\right.\right.\\&\times\left(M(\lambda)e^{-\xi_{11}L}-\frac{N(\lambda)}{1-B_{21}(\lambda)}\right)\\&\left.\left.+\frac{B_{21}(\lambda)}{1-B_{21}(\lambda)}\tilde{h}_2(\lambda,L)\right]\right\},\end{aligned} \tag{43}$$

and

$$\begin{aligned}E(\lambda)=\frac{1}{(1+B_{21})-(1-B_{21})e^{-2\xi_{11}L}}&\left\{\frac{2g(\lambda)}{e^{\xi_{11}L}}\right.\\&+\delta_1\left[2\left(\frac{q_{11}}{\xi_{11}}\right)M(\lambda)e^{-\xi_{11}L}-\left(\frac{q_{11}}{\xi_{11}}\right)\right.\\&\left.\left.\times(1+e^{-2\xi_{11}L})N(\lambda)-\tilde{h}_2(\lambda,L)(1-e^{-2\xi_{11}L})\right]\right\},\end{aligned} \tag{44}$$

where the following definitions were made for convenience:

$$\begin{aligned}M(\lambda)\equiv\frac{1}{1-e^{-2q_{11}L}}&[\tilde{h}_2(\lambda,0)(1+e^{-2q_{11}L})\\&-2\tilde{h}_2(\lambda,L)e^{-q_{11}L}],\end{aligned} \tag{45a}$$

and

$$\begin{aligned}N(\lambda)\equiv\frac{1}{1-e^{-2q_{11}L}}&[2\tilde{h}_2(\lambda,0)e^{-q_{11}L}\\&-\tilde{h}_2(\lambda,L)(1+e^{-2q_{11}L})].\end{aligned} \tag{45b}$$

According to the definition of $f(\rho,0)$, use of the expressions for $A(\lambda)$ and $B(\lambda)$ in Eq. (25) and the inverse Hankel transformations yields

$$\begin{aligned}f(\rho,0)=\frac{I_0w^2}{k_{10}\delta_2}&[\sqrt{1+2\delta_2F_{10}(\rho,0)}-1]\\&\times\int_0^\infty\left(\frac{1+\Gamma_{21}(\lambda)e^{-2\xi_{11}L}}{\xi_{11}(1-\Gamma_{21}(\lambda)e^{-2\xi_{11}L})}\right)\\&\times e^{-\lambda^2w^2/4}J_0(\lambda\rho)\lambda d\lambda.\end{aligned} \tag{46}$$

Finally, the nonlinear thermal-wave field can be found using Eq. (30) and the stepwise approximation, Eq. (38), for $H_2(\rho,z)$:

$$T_{11}(\rho,0)=H_1(\rho,0)-(\delta_1+\delta_2)f(\rho,0), \tag{47}$$

with

$$H_1(\rho,0)=\int_0^\infty \tilde{h}_1(\lambda,0)J_0(\lambda\rho)\lambda d\lambda$$

$$=\int_0^\infty [A(\lambda)+B(\lambda)]J_0(\lambda\rho)\lambda d\lambda. \quad (48)$$

In order to calculate the inverse Hankel transforms, the value of $\tilde{h}_2(\lambda,L)$ will also be required. From Eqs. (42) and (43) we derive the sum $A(\lambda)+B(\lambda)$ and, when taking Hankel transforms, we note that

$$\tilde{h}_2(\lambda,0)=\int_0^\infty f(\rho,0)J_0(\lambda\rho)\rho d\rho, \quad (49a)$$

and

$$\tilde{h}_2(\lambda,L)=\int_0^\infty f(\rho,L)J_0(\lambda\rho)\rho d\rho, \quad (49b)$$

where $f(\rho,0)$ is given by Eq. (46) and a similar treatment using Eq. (25) and inverting the Hankel transforms yields

$$f(\rho,L)=\frac{2I_0w^2}{k_{10}\delta_2}[\sqrt{1+2\delta_2F_{10}(\rho,L)}-1]$$

$$\times\int_0^\infty\left(\frac{1}{\xi_{11}(\lambda)[1+B_{21}(\lambda)][1-\Gamma_{21}(\lambda)e^{-2\xi_{11}L}]}\right)$$

$$\times e^{-\lambda^2w^2/4}J_0(\lambda\rho)\lambda d\lambda. \quad (50)$$

For computational purposes, for each value of the Hankel variable λ in Eqs. (49a) and (49b), the entire spectrum of the functions $f(\rho,0)$ and $f(\rho,L)$ must be calculated under the integral signs for $0\leqslant\rho<\infty$. Also, Eqs. (46) and (50) show that each such value of $f(\rho,0)$ and $f(\rho,L)$ is the result of complete numerical integrations over the Hankel variable λ. Therefore, operationally, the calculation of $H_1(\rho,0)$ requires numerical computation of $f(\rho,0)$ and $f(\rho,L)$ for each ρ from Eqs. (46) and (50), respectively, followed by integration over ρ, Eqs. (49a) and (49b), to produce each value of the spectra $\tilde{h}_2(\lambda,0)$ and $\tilde{h}_2(\lambda,L)$ which are needed for computing $\tilde{h}_1(\lambda,0)$. Finally, integration over all λ yields the desired $H_1(\rho,0)$ value. Symbolically,

$$\tilde{h}_2(\lambda,0)=\int_0^\infty f_1(\rho)\left[\int_0^\infty f_2(\lambda')J_0(\lambda'\rho)\lambda' d\lambda'\right]J_0(\lambda\rho)\rho d\rho,$$

and

$$\tilde{h}_2(\lambda,L)=\int_0^\infty f_1(\rho)\left[\int_0^\infty f_3(\lambda')J_0(\lambda'\rho)\lambda' d\lambda'\right]J_0(\lambda\rho)\rho d\rho,$$

where $f_1(\rho)$ is the (common) functional form of $f(\rho,0)$, Eq. (46) and $f(\rho,L)$, Eq. (50), before the integral sign, and $f_2(\lambda)$, $f_3(\lambda)$ are the λ-dependent terms in brackets under the integral signs of $f(\rho,0)$ and $f(\rho,L)$, respectively.

Finally, for the nonlinear thermal-wave field at the fundamental angular frequency ω we obtain from Eq. (47),

$$T_{11}(\rho,0)=[1-(\delta_1+\delta_2)T_{10}(\rho,0)]H_{10}(\rho,0)+\delta_1R(\rho), \quad (51)$$

where $H_{10}(\rho,0)$ is given by Eq. (37) with $z=0$; $T_{10}(\rho,0)$ is the dc term given by Eq. (19) with $z=0$ and

$$R(\rho)\equiv\int_0^\infty\frac{J_0(\lambda\rho)\lambda d\lambda}{1-\Gamma_{21}(\lambda)e^{-2\xi_{11}L}}\left\{\left(\frac{q_{11}(\lambda)}{\xi_{11}(\lambda)}\right)\right.$$

$$\times\left[M(\lambda)(1+\Gamma_{21}(\lambda)e^{-2\xi_{11}L})-\frac{2N(\lambda)}{1+B_{21}(\lambda)}e^{-\xi_{11}L}\right]$$

$$\left.+\frac{2B_{21}(\lambda)}{1+B_{21}(\lambda)}\tilde{h}_2(\lambda,L)e^{-\xi_{11}L}\right\}, \quad (52)$$

where $M(\lambda)$ is given by Eq. (45a), $N(\lambda)$ is given by Eq. (45b), $\tilde{h}_2(\lambda,0)$ is given by Eqs. (49a) and (46), and $\tilde{h}_2(\lambda,L)$ is given by Eqs. (49b) and (50).

Equation (51) is the central result of the present work. Along with the corresponding formulas, Eqs. (37), (19), and (52), it describes the radial distribution of the fundamental temperature field on the surface of a thin layer with nonlinear thermal conductivity and specific heat. In Sec. III we discuss some very interesting features and limiting cases of the general theoretical model.

Note, that by using master equations (8a) and (8b) for the nonlinear thermal-wave field, the governing equations for all higher harmonic responses (second, third, etc.) can be found. For instance, the second harmonic field is described by the boundary-value problem comprising

$$\nabla^2\{[1+\delta_2T_{10}(\mathbf{r})]T_{12}(\mathbf{r})+\tfrac{1}{2}\delta_2T_{11}^2(\mathbf{r})\}$$

$$-\sigma_{12}^2\{[1+\delta_1T_{10}(\mathbf{r})]T_{12}(\mathbf{r})+\tfrac{1}{2}\delta_1T_{11}^2(\mathbf{r})\}=0 \quad (53a)$$

for the upper layer, and

$$\nabla^2T_{22}(\mathbf{r})-\sigma_{22}^2T_{22}(\mathbf{r})=0 \quad (53b)$$

for the substrate. Here $T_{10}(\mathbf{r})$ and $T_{11}(\mathbf{r})$ are the fields given by Eqs. (19) and (51), respectively. The harmonic wave vectors are given by

$$\sigma_{12}^2=2i\omega/\alpha_{10}, \quad \sigma_{22}^2=2i\omega/\alpha_2. \quad (54)$$

The flux boundary condition at $z=0$ can be derived from Eq. (5a):

$$-k_0\frac{\partial}{\partial z}\{T_{12}(\mathbf{r})+\tfrac{1}{2}\delta_2[T_{11}^2(\mathbf{r})+2T_{10}(\mathbf{r})T_{12}(\mathbf{r})]\}\big|_{z=0}=0. \quad (55)$$

III. DISCUSSION

A. Temperature-dependent thermal conductivity or specific heat

Equation (51) gives the fundamental nonlinear thermal-wave profile for the case where both the thermal conductivity and the specific heat of the upper layer are temperature dependent. Let us assume now that only the thermal conductivity varies with temperature. Letting $\delta_1=0$ in Eq. (51) and using Eq. (19) for $T_{10}(\rho,0)$ we obtain, after a few algebraic operations,

$$T_{\mathrm{NL}}(\rho,0)=T_L(\rho,0)[2-\sqrt{1+\delta_2F_{10}(\rho,0)}], \quad (56)$$

where $T_{\mathrm{NL}}(\rho,0)$ is the nonlinear temperature field $T_{11}(\rho,0)$, $T_L(\rho,0)=H_{10}(\rho,0)$, etc. This term represents the linear fundamental thermal-wave field, and $F_{10}(\rho,0)$ is defined by Eq. (17) with $z=0$.

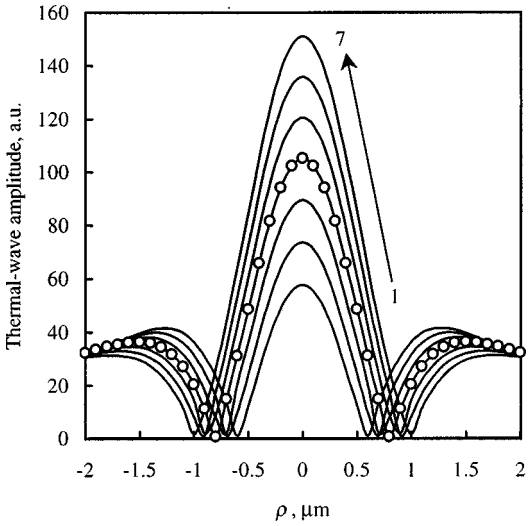

FIG. 2. Fundamental thermal-wave amplitude lateral profiles calculated using Eq. (56) for different ratios of the thermal conductivities of the nonlinear layer ($L=0.5\ \mu$m) and the linear substrate: (1) $k_{10}/k_2=0.7$; (2) 0.8; (3) 0.9; (4) 1.0; (5) 1.1; (6) 1.2; and (7) 1.3. The points represent a semi-infinite nonlinear sample. The parameters used for the calculations were $k_{10}=1.7$ W/cm K, $I_0=2$ MW/cm^2, $w=0.6\ \mu$m, $f=1$ MHz and $\delta_2=5\times10^{-3}$ K^{-1}.

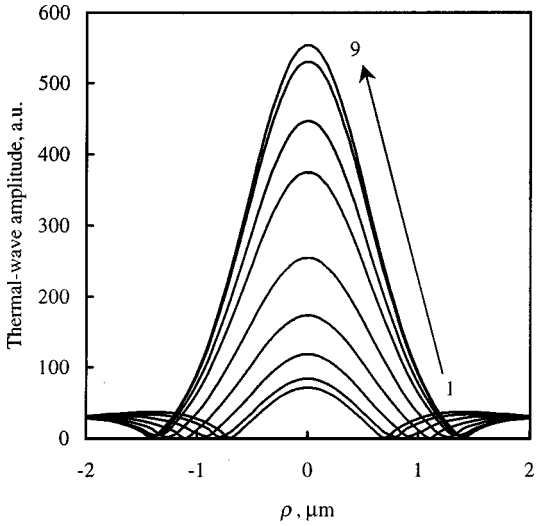

FIG. 3. Fundamental thermal-wave amplitude lateral profiles calculated using Eq. (56) for a system of a linear substrate and a nonlinear overlayer [$k(T)$ only, $\delta_1=0$] of various thicknesses: (1) $L=10$, (2) 2.5, (3) 1.0, (4) 0.5, (5) 0.25, and (6) 0.1 μm and (7) 500, (8) 100, and (9) 10 Å. The parameters used for the calculations were $k_{10}=1.7$ W/cm K and $k_2=0.85$ W/cm K. The other parameters are the same as in Fig. 2.

Since $F_{10}(\rho,0)$ is a real function, the first important conclusion is that the nonlinearities in the upper layer thermal conductivity do not affect the phase of the fundamental thermal-wave field. Both $T_{\mathrm{NL}}(\rho,0)$ and $T_L(\rho,0)$ temperature fields have the same (linear) phase.

Another interesting observation for the $k(T)$-only case is that, if the unperturbed layer conductivity k_{10} and substrate conductivity k_2 are equal and so are the corresponding thermal diffusivities α_{10} and α_2, then the two layers merge thermally into one, semi-infinite nonlinear layer. Indeed, if we let $k_{10}=k_2$ and $\alpha_{10}=\alpha_2$, then from the definition of the dc-field thermal coupling coefficient b_{21} we obtain $\gamma_{21}=0$ and from the ac-field thermal coupling coefficient, Eq. (36), it follows that $B_{21}(\lambda)=1$, $\Gamma_{21}(\lambda)=0$. Therefore, the resulting nonlinear thermal-wave field $T_{\mathrm{NL}}(\rho,0)=T_{11}(\rho,0)$ becomes independent of L.

In other words, if only the thermal conductivity exhibits nonlinear behavior, and if the unperturbed thermal conductivity and diffusivity of the upper nonlinear layer are equal to those of the substrate, there is no way to define the characteristic depth of the thermal conductivity nonlinearities (e.g., layer thickness L). The entire system behaves like one semi-infinite nonlinear layer.

Figure 2 illustrates the aforementioned behavior of the nonlinear thermal-wave field in the case of temperature-dependent thermal conductivity only. With fixed thickness of the overlayer the nonlinear thermal-wave amplitude has distinct lateral profiles as long as $k_{10}\neq k_2$ and becomes identical to that of a semi-infinite nonlinear sample with the same parameters when $k_{10}=k_2$ [curve (4) in Fig. 1]. The amplitude minima seen in Figs. 2 and 3 are due to thermal-wave interference in the radial direction when the upper nonlinear layer confines the thermal energy. This interference pattern becomes narrower with decreasing ratio k_{10}/k_2 (Fig. 2) and decreasing thickness of the nonlinear overlayer (Fig. 3). For different thermal conductivities between the overlayer and the substrate, the resulting nonlinear thermal-wave field maintains its dependence on L, as expected (Fig. 3).

It is interesting to note that the thinner the nonlinear layer is, the stronger its effect on the thermal-wave amplitude becomes. This occurs due to the more effective confinement of thermal energy within a thinner layer, which enhances (amplifies) the nonlinear nature of the layer. Experimentally, this feature of the thermal-wave response of nonlinear surface layers should make their laser photothermal diagnostics easier than their linear counterparts. This signal amplification property of confined nonlinear thermal waves has already been established in preliminary experimental studies.[4,11]

In the case of temperature-dependent specific heat only, by letting $\delta_2=0$ in Eq. (51) we obtain

$$T_{\mathrm{NL}}(\rho,0)=T_L(\rho,0)(1-\delta_1F_{10}(\rho,0))+\delta_1R'(\rho), \qquad (57)$$

where $R'(\rho)$ is defined by Eq. (52) with $q_{11}(\lambda)=\lambda$. Since $R'(\rho)$ is a complex function, unlike the previous case of nonlinear thermal conductivity only, nonlinearities in the specific heat of the upper layer affect both the amplitude and the phase of the fundamental thermal-wave field. Correspondingly, any experimentally observed deviation in the phase behavior with respect to that predicted by a linear model will indicate the contribution from the temperature-dependent specific heat.

Unlike the previous $k(T)$-only case, it can be shown that the nonlinear thermal-wave field here is always L dependent and that the nonlinearities in the specific heat of the upper layer have a characteristic depth regardless of the ratios k_{10}/k_2 and α_{10}/α_2. As an example, if we put $\delta_2=0$ and $k_{10}=k_2$, then from the definition of the corresponding functions in Eq. (52) we obtain

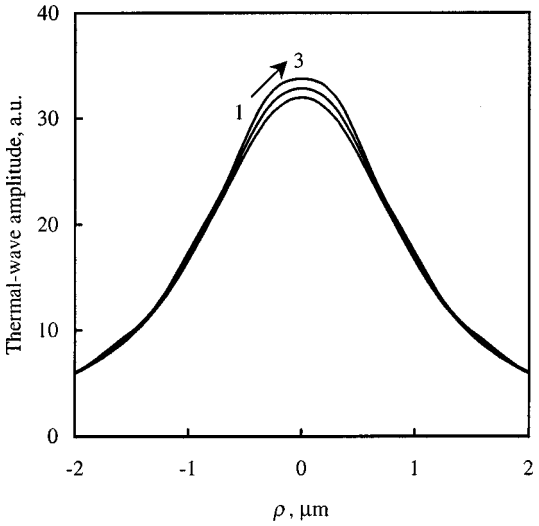

FIG. 4. Fundamental thermal-wave amplitude lateral profiles calculated for a system of a linear substrate and a nonlinear overlayer [$C(T)$ only, $\delta_2=0$] of various thicknesses: (1) $L=500$, (2) 50, and (3) 25 Å. The parameters used for the calculations were $k_{10}=k_2=1.7$ W/cm K and $\delta_1=1\times10^{-5}$ K^{-1}. The other parameters are the same as in Fig. 2.

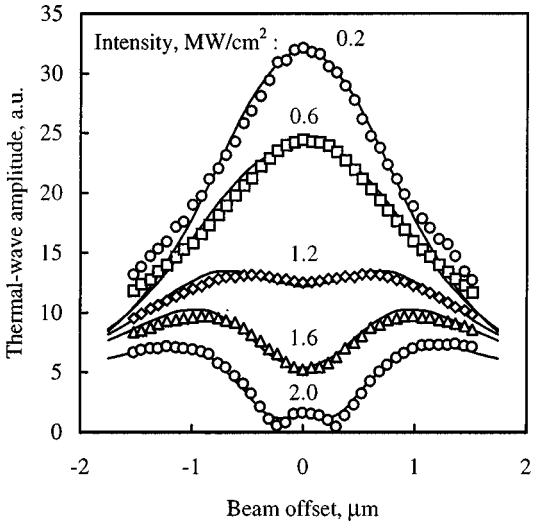

FIG. 5. Experimental fundamental thermal-wave amplitude lateral profiles obtained for a 3000 Å tungsten layer at different pump beam intensities (points), and the results of fitting to the theoretical model (lines).

$$R(\rho)=\int_0^\infty \frac{J_0(\lambda\rho)\lambda^2 d\lambda}{\xi_{11}(\lambda)}Q(\lambda,L),$$

where $Q(\lambda,L)$ is a dimensionless function that always depends on L.

In Fig. 4 the nonlinear lateral profiles of the thermal-wave amplitude calculated for $k_{10}=k_2$ are plotted for various thicknesses of the overlayer. As expected from the foregoing considerations, in the case of temperature dependent specific heat only, the nonlinear thermal-wave field is always L dependent, even with $k_{10}=k_2$ and $\alpha_{10}=\alpha_2$. This feature is expected to improve the laser photothermal sensitivity of a nonlinear thin layer over a geometrically similar linear thin layer. It can be concluded that both $k(T)$ and $C(T)$ nonlinearities tend to enhance the contrast between thin surface layers and substrates, thus improving the dynamic reserve of photothermal detection.

Preliminary experimental results validating the present theoretical model have been obtained using a photothermal experimental system[12] that measures the lateral profile of the thermal-wave field using the photomodulated thermoreflectance technique. Thermal-wave lateral scans have been measured on a set of silicon wafers containing tungsten overlayers of various thicknesses at different intensities of the pump beam at a modulation frequency of 1 MHz.

Figure 5 shows the experimental amplitude lateral scans recorded for the thinnest tungsten layer of 3000 Å. The nonlinearities introduced by the thin tungsten overlayer result in dramatic changes in the shape of the amplitude lateral scans which exhibit a characteristic wave-like behavior as predicted by the theoretical model. The increasing nonlinearity tends to couple more power into the harmonic spectrum and out of the fundamental, so the amplitude of the fundamental photothermal response in Fig. 5 decreases with increasing intensity of the pump beam.

The results of the best fit to the present theoretical model are also shown in Fig. 5. All amplitude lateral scans recorded at different pump beam intensities have been fitted simultaneously using the same set of fitting parameters. As can be seen from Fig. 5, the experimental and theoretical results are in very good agreement. It has been found that the nonlinear behavior observed for this sample is mostly due to the nonlinear thermal conductivity of the tungsten layer. Fitting revealed $\delta_2=4.5\times10^{-3}$ K^{-1} and $\delta_1=2\times10^{-5}$ K^{-1}. The same nonlinear behavior of the thermal-wave field with decreasing effective nonlinear parameter δ_2 (and practically unchanged δ_1) was observed for the rest of the wafers from this set (Fig. 6). A more complete experimental study of the nonlinear tungsten layers will be presented in a separate publication.

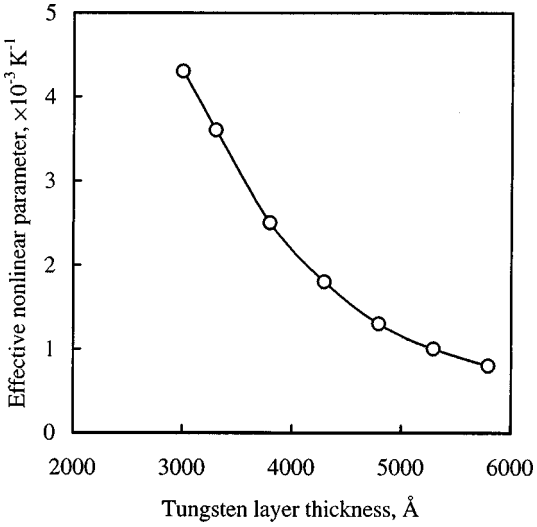

FIG. 6. Effective nonlinear parameter δ_2 as a function of tungsten layer thickness obtained by fitting of the experimental lateral scans.

B. Limiting cases of the model

1. $L \to \infty$

For a semi-infinite nonlinear upper layer Eq. (51) and the accompanying formulas can be simplified. Taking the limit $L \to \infty$ after some algebra we obtain

$$T_{11}(\rho,0) = [1-(\delta_1+\delta_2)T_0(\rho,0)]H_0(\rho,0) + \delta_1 \int_0^\infty \frac{q_1(\lambda)G(\lambda)}{\xi_1(\lambda)} J_0(\lambda\rho)\lambda d\lambda, \tag{58}$$

where, from Eq. (19),

$$T_0(\rho,0) = \frac{1}{\delta_2}[\sqrt{1+2\delta_2 F_0(\rho,0)}-1], \tag{59}$$

with

$$F_0(\rho,0) = \frac{I_0 w^2}{k_{10}} \int_0^\infty e^{-\lambda^2 w^2/4} J_0(\lambda\rho) d\lambda \tag{60}$$

from Eq. (17), and

$$H_0(\rho,0) = \frac{I_0 w^2}{k_{10}} \int_0^\infty \frac{J_0(\rho\lambda) e^{-\lambda^2 w^2/4} \lambda d\lambda}{\xi_1(\lambda)} \tag{61}$$

from Eq. (37).

Also from the definition of $R(\rho)$ in Eq. (52) one may write in Eq. (58)

$$G(\lambda) = \int_0^\infty F_2(\rho) J_0(\lambda\rho)\rho d\rho, \tag{62}$$

where $F_2(\rho) = T_0(\rho,0)H_0(\rho,0)$, or, explicitly,

$$F_2(\rho) = \frac{I_0 w^2}{k_{10}\delta_2}[\sqrt{1+2\delta_2 F(\rho,0)}-1] \times \int_0^\infty \frac{e^{-\lambda^2 w^2/4} J_0(\lambda\rho)\lambda d\lambda}{\xi_1(\lambda)}. \tag{63}$$

In the foregoing expressions k_{10} and α_{10} stand for the unperturbed thermal conductivity and diffusivity of the sample, and

$$\xi_1(\lambda) = \sqrt{\lambda^2+\sigma_1^2}, \quad \sigma_1^2 = i\omega/\alpha_{10}. \tag{64}$$

The nonlinear thermal-wave field amplitude and phase lateral profiles calculated for a semi-infinite nonlinear sample are presented in Fig. 7 along with the corresponding linear responses. Similar to the case of the two-layer system discussed earlier, the temperature-dependent thermal conductivity only affects the amplitude profile while the phase remains the same as for the linear sample [Fig. 7(b)]. The nonlinear specific heat affects both the amplitude and the phase behavior, and in the case of $\delta_1, \delta_2 \neq 0$ both the amplitude and the phase of the nonlinear thermal-wave field exhibit very strong deviations from their conventional linear profiles.

2. $L \to 0$

Another limiting case of interest regarding the general two-layer model is that of an infinitely thin upper nonlinear layer. Setting $L=0$ at $z=0$ in Eq. (17) we obtain

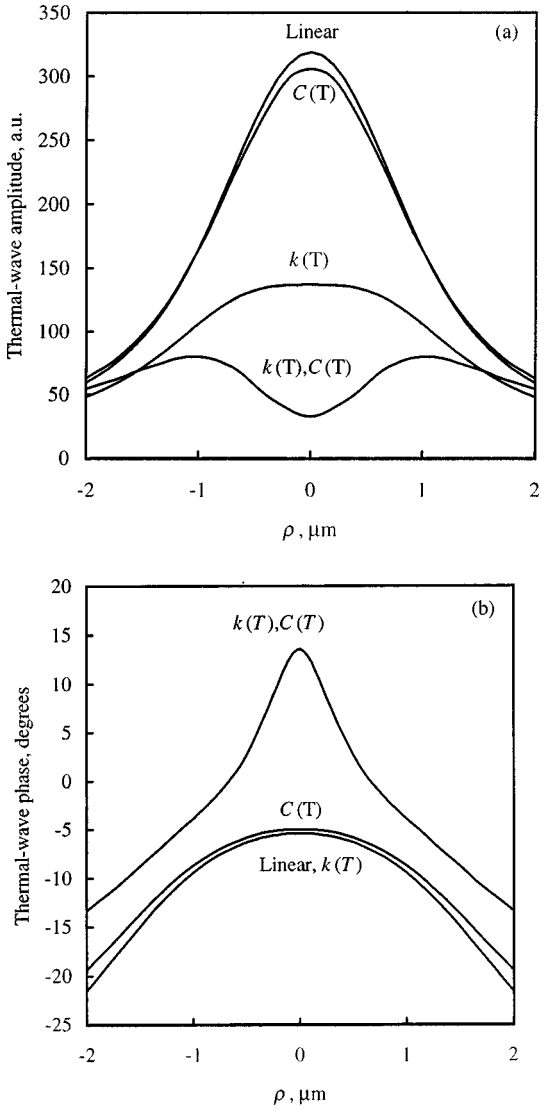

FIG. 7. Fundamental thermal-wave amplitude (a) and phase (b) lateral profiles calculated for a semi-infinite nonlinear sample with the following nonlinear parameters: $\delta_1 = 1\times10^{-5}\ \mathrm{K}^{-1}$; $\delta_2 = 4\times10^{-3}\ \mathrm{K}^{-1}$. The other parameters are the same as in Fig. 2, and $\alpha_0 = 0.7\ \mathrm{cm}^2/\mathrm{s}$. Also shown are the amplitudes and phases for (i) a linear sample ($\delta_1=\delta_2=0$), (ii) a sample with $k(T)$ only ($\delta_1=0$), and (iii) a sample with $C(T)$ only ($\delta_2=0$).

$$F_{10}(\rho,0) = \frac{I_0 w^2}{k_2} \int_0^\infty e^{-\lambda^2 w^2/4} J_0(\lambda\rho) d\lambda. \tag{65}$$

This field represents a dc surface temperature radial distribution. The only material present on the right-hand side of Eq. (65) is the substrate (k_2). From Eq. (18), for the underlying substrate's dc temperature response to a Gaussian laser beam we also obtain

$$T_{20}(\rho,z) = \frac{I_0 w^2}{k_2} \int_0^\infty e^{-\lambda z} e^{-\lambda^2 w^2/4} J_0(\lambda\rho) d\lambda, \quad L \leqslant z < \infty. \tag{66}$$

This equation shows that $T_{20}(\rho,z)$ behaves like a semi-infinite solid with thermal conductivity k_2 and no overlayer. Equation (66) is identical to Eq. (60) of a single semi-infinite nonlinear layer once one sets $z=L=0$. Taking the relation between $T_0(\rho,0)$ and $F_0(\rho,0)$ given by Eq. (59), we note,

however, that this equation reduces to the actual dc temperature field of a linear semi-infinite solid only by setting $\delta_2 = 0$. Then, the dc terms $F_{10}(\rho,z)$ and $T_{20}(\rho,z)$ of the two-layer treatment reduce to $F(\rho,0)$ and $F(\rho,z)$, respectively, when $L=0$. It is seen that they assume the meaning of the surface and bulk temperature of a linear semi-infinite solid only if $\delta_2=0$ is imposed in addition to $L=0$.

In other words, the seemingly peculiar situation arises in which to eliminate the effects of the upper nonlinear layer it is not enough to set $L=0$; the nonlinearities must also vanish. For the dc term one must set $\delta_2=0$. The *mathematical reason* is that with even an extremely thin nonlinear surface layer first intercepting the incident radiation modulated at angular frequency ω, the incident converted optical-to-thermal power becomes automatically partitioned to a series of harmonics of the fundamental frequency: the thin film acts as a frequency multiplexer which subsequently feeds energy into the linear substrate at the fundamental frequency and all its harmonics, with efficiency dependent on the magnitudes of δ_1 and/or δ_2. This is very different from imparting all the incident power just into the dc temperature and the fundamental thermal-wave response of a single layered linear solid and is similar to mechanisms driving other nonlinear fields, e.g., acousto-optic effects. *Mathematically*, from Eq. (7), $T_2(\mathbf{r},t)$ can never be equal to $T_{21}(\mathbf{r})e^{i\omega t}$ only, unless $T_{20}(\mathbf{r})=T_{22}(\mathbf{r})=\ldots=0$; but these terms arise from $\delta_1,\delta_2 \neq 0$ and putting them equal to zero without putting $\delta_1=\delta_2=0$ results in inconsistency.

Based on this argument, it is easy to understand that in order to eliminate all substrate harmonics one must set $\delta_1=\delta_2=0$, otherwise conservation of incident flux is violated. Under these conditions Eq. (51) then reduces to

$$T_{11}(\rho,0)=H_{10}(\rho,0). \tag{67}$$

Now, letting $L=0$ in Eq. (37) after some manipulation we obtain

$$H_{10}(\rho,0)=\frac{I_0 w^2}{k_2}\int_0^\infty \frac{J_0(\rho\lambda)e^{-\lambda^2 w^2/4}\lambda\, d\lambda}{\sqrt{\lambda^2+i\omega/\alpha_2}}. \tag{68}$$

This equation for a linear substrate is identical to Eq. (61) valid for a single linear layer with thermal properties equal to those of the substrate (k_2), as expected.

Physically, the nonzero nonlinear constants of a thin upper layer, δ_1 and δ_2, are responsible for the dependence of the two thermophysical parameters $C(T)$ and $k(T)$ on the temperature *increment* across the thickness of the thin film, Eqs. (3a) and (3b). It is thus possible for a portion of the incident thermal power to be stored in the nonlinear components of these properties without raising the incremental temperature of the film. Since $\delta_1,\delta_2\to 0$ is tantamount to $T_1(\mathbf{r},t)\to 0$ in Eqs. (3a) and (3b), the existence of nonzero nonlinear constants artificially sustains a nonzero virtual temperature increment across the film thickness, even when $L=0$. Therefore, the more physically correct manner in which to approach the $L\to 0$ case is to require independently that $\delta_1=\delta_2=0$ for consistency. This condition annuls the storing of energy in the nonlinear thermophysical modes of the upper layer and fully erases its ''memory'' when $L=0$.

The very interesting conclusion of the foregoing considerations is the persistence of the efficiency of the thin nonlinear layer as an energy conversion filter which, in principle, drives the harmonic response of the substrate even as $L=0$. In actual simulations (and measurements), the effect of very thin upper layers may be too small to make a numerical difference, unless δ_1 or δ_2 is so strong that one of them channels the incident flux to harmonics in proportions beyond the effects of the thermal mass (i.e., the fundamental thermal impedance) of the upper layer. In this circumstance the thermal-mass effect vanishes with L, but the harmonic channeling efficiency does not vanish linearly with L, so that the product $\delta_j T$ remains finite for all nonzero values of the surface temperature, even when $L=0$. In this case the temperature of the upper layer becomes identical to that of the substrate. These considerations indicate that the effects of nonlinearity in the thermal-wave behavior of solids may be particularly stronger than the weight of their thermal masses, as indicated in Fig. 3.

IV. CONCLUSIONS

A three-dimensional theoretical model of the photothermal response in a solid layer with nonlinear thermophysical properties (thermal conductivity and specific heat) has been presented. The solid layer was assumed to lie on a semi-infinite backing with linear thermophysical properties. It was shown that the photothermal boundary-value problem is equivalent to the superposition of an infinite set of boundary-value problems, each problem being associated with a particular harmonic of the incident optical radiation modulation frequency ω, including the dc temperature rise and the fundamental response at ω. The theory used a stepwise approximation to the exact solution, akin to the Born approximation in scattering field theory, and the fundamental response was highlighted as the experimentally relevant signal channel. Expressions for the fundamental thermal-wave field were derived and the special cases of either conductivity or specific heat nonlinearities were studied. The role of the nonlinear layer as a thermal-wave frequency multiplexing medium even in the limit of very thin overlayers has been investigated. Preliminary experimental results obtained using the photomodulated thermoreflectance technique were presented as validation of the nonlinear theory, and the nonlinear parameter δ_2 was calculated for a thin tungsten layer that exhibited a strong nonlinear behavior.

ACKNOWLEDGMENT

One of the authors (A.M.) wishes to acknowledge the partial support of the Natural Sciences and Engineering Research Council of Canada (NSERC) through a research grant.

[1] See, for example, A. Rosencwaig, *Photoacoustics and Photoacoustic Spectroscopy* (Wiley, New York, 1980); *Principles and Perspectives of Photothermal and Photoacoustic Phenomena*, edited by A. Mandelis (Elsevier, New York, 1992), Vol. I.
[2] *Photoacoustic and Thermal Wave Phenomena in Semiconductors*, edited by A. Mandelis (North-Holland, New York, 1987).
[3] J. Opsal, A. Rosencwaig, and D. Willenborg, Appl. Opt. **22**, 3169 (1983).

[4] Y. N. Rajakarunanayake and H. K. Wickramasinghe, Appl. Phys. Lett. **48**, 218 (1986).
[5] G. C. Wetsel and J. B. Spicer, Can. J. Phys. **64**, 1269 (1986).
[6] O. Doka, A. Miklos, and A. Lorincz, Appl. Phys. A: Solids Surf. **48**, 415 (1989).
[7] C. Wang and P. Li, J. Appl. Phys. **74**, 5713 (1993).
[8] V. Gusev, A. Mandelis, and R. Bleiss, Mater. Sci. Eng., B **26**, 111 (1993).
[9] V. Gusev, A. Mandelis, and R. Bleiss, Int. J. Thermophys. **14**, 321 (1993).
[10] V. Gusev, A. Mandelis, and R. Bleiss, Appl. Phys. A: Solids Surf. **57**, 229 (1993).
[11] S. B. Peralta, H. H. Al-Khafaji, and A. W. Williams, Nondestr. Test. Eval. **6**, 17 (1991).
[12] L. Chen, A. Salnick, J. Ding, M. Hovinen, H. Chu, J. Opsal, and A. Rosencwaig, Technical Abstracts of the *X* International Conference on Photoacoustic and Photothermal Phenomena, August 1998, Rome, Italy, p. 69.